CAUCHY – Jurnal Matematika Murni dan Aplikasi
Volume 10 (2) (2025), Pages 1361-1371
p-ISSN: 2086-0382; e-ISSN: 2477-3344

Development of a Fuzzy Logic Model for Tsunami Early Detection Using TUNAMI F1 on the Southern Coast of Yogyakarta International Airport

Sadiyana Yaqutna Naqiya[1], Hanah Khoirunnisa[2], and Galih Pradananta[3*]

[1]*Department of Mathematics, School of Mathematics and Science, Republic of Indonesia Defense University, Indonesia*
[2]*Research Center for Hydrodynamics, BRIN, Yogyakarta, Indonesia*
[3]*Department of Mathematics, UIN Sayyid Ali Rahmatullah Tulungagung, Indonesia*

Abstract

Tsunami disaster mitigation requires a reliable early warning system to reduce traumatic impacts and material losses. This study develops a fuzzy logic model for early tsunami detection by integrating sea surface height (SSH) and estimated tsunami arrival time (ETATSU) parameters. The model is combined with the TUNAMI F1 simulation, which considers seabed topography and fluid dynamics. Simulations were conducted on 36 earthquake scenarios on the southern coast near Yogyakarta International Airport (YIA). The results show that the model successfully classifies tsunami risks into three categories: *alert*, *standby*, and *emergency*, with an overall accuracy of 83.3%. Some scenarios show invalid results at high magnitudes ($M_w \geq 8.5$). This research improves the accuracy of tsunami early warning systems, potentially saving more lives and minimizing the impact of disasters.

Keywords: fuzzy logic; early warning tsunami; F1 TUNAMI model.

1 Introduction

Tsunami early detection is crucial for disaster mitigation to reduce traumatic impacts and material losses [1]. The fuzzy logic-based approach offers adaptive capabilities in handling seismic and oceanographic data uncertainty. Previous studies have used single parameters such as volcanic eruptions, earthquakes, landslides, or sea surface height. Still, few have integrated two key parameters, namely sea surface height (SSH) and estimated tsunami arrival time (ETATSU) [2].

The fuzzy logic model consists of three main components: fuzzification, inference system, and defuzzification [3]. Fuzzification transforms data, such as sea surface height, into categories like `low`, `medium`, or `high`, while the inference system processes the data based on `if-then` rules [4].

The defuzzification process produces numerical output that is used for tsunami warnings. The advantages of this model include flexibility in modifying rules, integration of multi-source data such as seismic sensors and satellite data, and the ability to provide quick and accurate warnings [5, 6].

*Corresponding author. E-mail: g.pradananta@uinsatu.ac.id

Submitted: July 11, 2025 Reviewed: September 02, 2025 Accepted: November 14, 2025
DOI: https://doi.org/10.18860/cauchy.v10i2.35416

Simulations using TUNAMI F1, a numerical model that accounts for seabed topography and fluid dynamics, help predict tsunami wave behavior accurately [7]. Through quick simulations and high resolution, TUNAMI F1 supports the analysis of tsunami behavior from the epicenter to the shore [8]. The integration of fuzzy logic with TUNAMI F1 is expected to produce a more reliable early warning system, saving lives and reducing the impact of disasters [9], [10].

Conventional approaches to early tsunami detection often rely on a single parameter such as sea surface height, tsunami arrival time, or earthquake characteristics (volcanic eruptions, landslides). Although these single parameters are helpful, they have limitations in addressing the complexity of tsunami phenomena. For instance, sea surface height alone is insufficient to determine risk as it does not account for how quickly the tsunami reaches the shore. On the other hand, estimated arrival time alone does not reflect the level of damage that may occur. Such approaches tend to yield less accurate detections or ineffective early warnings, especially in complex disaster scenarios.

This study provides a new contribution by combining two key parameters, namely sea surface height or sea surface height (SSH) and estimated tsunami arrival time (ETATSU), into a fuzzy logic-based model. This integration allows for a more comprehensive risk analysis, where the relationship between tsunami speed and potential damage can be assessed simultaneously. Furthermore, using TUNAMI F1 simulations as a supporting tool for the fuzzy logic model provides a reliable numerical framework for validating results. Through this approach, the study not only enhances the accuracy of early warning systems but also introduces an adaptive framework that can be applied to other coastal regions.

To guide the flow of this paper, the remaining sections are organized as follows. Section 2 describes the methodological framework, including the construction of initial water surface conditions and the numerical simulation setup using the TUNAMI F1 model. Section 3 presents the simulation outcomes and discusses the performance of the fuzzy logic model in classifying tsunami risk levels across different earthquake scenarios. Section 4 summarizes the key findings and outlines recommendations for future development of tsunami early warning systems.

2 Methods

In this section, we outline the methodological framework used to generate tsunami scenarios and derive the input parameters for the fuzzy logic early warning model. Earthquake source parameters are first used to construct initial water surface conditions, which are then simulated with the TUNAMI F1 model to obtain SSH and ETATSU at selected observation and sensor points. The following subsections describe the setup of these simulations and the resulting data that support the analysis in Section 3.

2.1 Modeling of Initial Water Surface Conditions

This subsection describes the process of constructing the initial water surface conditions used in the tsunami simulations. The procedure consists of three main components: (1) defining the modeling domain, (2) determining the earthquake source parameters based on the Scaling Law, and (3) generating the initial seafloor deformation that triggers the tsunami waves.

Modeling Domain

All simulations were carried out within a fixed geographic domain covering the southern coastal region of Yogyakarta International Airport (YIA). The longitudinal and latitudinal boundaries of this domain are listed in Table 1. This spatial extent forms the computational grid for the TUNAMI F1 model and ensures that all epicenter scenarios fall within or adjacent to the region of interest.

Table 1: Modeling Area Boundaries

Longitude	**Latitude**
103.928734	-6.402655
114.828952	-11.786096

Earthquake Source Parameters

The tsunami scenarios were constructed using earthquake source parameters derived from the Scaling Law by [11]. Each scenario is characterized by the earthquake magnitude Mw, epicenter location, focal depth, and fault geometry—defined through strike, dip, and slip angles. The rupture length L and rupture width W describe the fault-plane dimensions, while the displacement D represents the maximum seafloor uplift or subsidence. These parameters collectively define the initial seafloor deformation that initiates the tsunami wave. The complete set of 36 scenarios used in this study is shown in Table 2.

Table 2: 36 Earthquake Parameter Scenarios [11].

Mw	Longitude	Latitude	Depth (km)	Strike	Dip	Slip	L (km)	W (km)	D (m)
7.0	106.578	-9.017	13.5	295.0	7.1	90	41.7	20.4	3.5
7.3	106.578	-9.017	13.8	295.1	7.3	90	58.9	26.0	5.4
7.6	106.578	-9.017	13.6	294.2	7.2	90	83.2	33.1	8.6
7.9	106.578	-9.017	13.6	294.2	7.1	90	117.5	42.2	13.5
8.2	106.578	-9.017	13.8	293.2	7.2	90	166.0	53.7	20.7
8.5	106.578	-9.017	14.3	291.7	7.4	90	234.4	68.4	31.2
7.0	106.904	-8.300	28.3	295.5	11.9	90	41.7	20.4	1.4
7.3	106.904	-8.300	28.3	295.5	11.9	90	58.9	26.0	2.2
7.6	106.904	-8.300	28.3	295.5	12.0	90	83.2	33.1	3.4
7.9	106.904	-8.300	28.2	295.7	12.1	90	117.5	42.2	5.4
8.2	106.904	-8.300	28.0	296.5	12.4	90	166.0	53.7	8.6
8.5	106.904	-8.300	27.8	297.9	12.7	90	234.4	68.4	13.5
7.0	107.967	-9.497	11.7	288.6	5.3	90	41.7	20.4	4.2
7.3	107.967	-9.497	11.7	288.1	5.3	90	58.8	26.0	6.7
7.6	107.967	-9.497	11.9	287.5	5.5	90	83.2	33.1	10.1
7.9	107.967	-9.497	11.8	286.7	5.5	90	117.5	42.2	16.1
8.2	107.967	-9.497	12.0	285.4	5.6	90	166.0	53.7	24.8
8.5	107.967	-9.497	12.5	283.7	6.1	90	234.4	68.4	36.8
7.0	109.730	-8.800	37.3	277.8	22.5	90	41.7	20.4	1.0
7.3	109.730	-8.800	37.3	277.9	22.4	90	58.9	26.0	1.6
7.6	109.730	-8.800	37.5	278.1	22.4	90	83.2	33.1	2.4
7.9	109.730	-8.800	37.2	279.1	22.0	90	117.5	42.2	3.8
8.2	109.730	-8.800	37.2	280.0	21.8	90	166.0	53.7	6.0
8.5	109.730	-8.800	37.2	281.0	21.4	90	234.4	68.4	9.4
7.0	112.119	-10.256	10.2	281.9	5.3	90	41.7	20.4	5.0
7.3	112.119	-10.256	10.3	281.9	5.4	90	58.9	26.0	7.8
7.6	112.119	-10.256	10.0	281.7	5.2	90	83.2	33.1	12.6
7.9	112.119	-10.256	10.4	282.4	5.5	90	117.5	42.2	18.9
8.2	112.119	-10.256	10.3	282.6	5.5	90	166.0	53.7	30.0
7.0	112.233	-9.255	31.4	283.6	18.7	90	41.7	20.4	1.2
7.3	112.233	-9.255	31.7	283.9	18.7	90	58.9	26.0	1.9
7.6	112.233	-9.255	30.9	284.2	18.3	90	83.2	33.1	3.1
7.9	112.233	-9.255	31.9	284.0	18.7	90	117.5	42.2	4.6
8.2	112.233	-9.255	32.4	284.2	18.7	90	166.0	53.7	7.1
8.5	112.233	-9.255	33.3	284.4	18.8	90	234.4	68.4	10.8

Epicenter Distribution and Observation–Sensor Configuration

The selected epicenter locations were mapped onto the modeling domain to represent six distinct source regions. Figure 1 shows the spatial arrangement of these epicenters, while Figure 2 illustrates the positions of observation and sensor points used to compare actual coastal conditions with offshore detections.

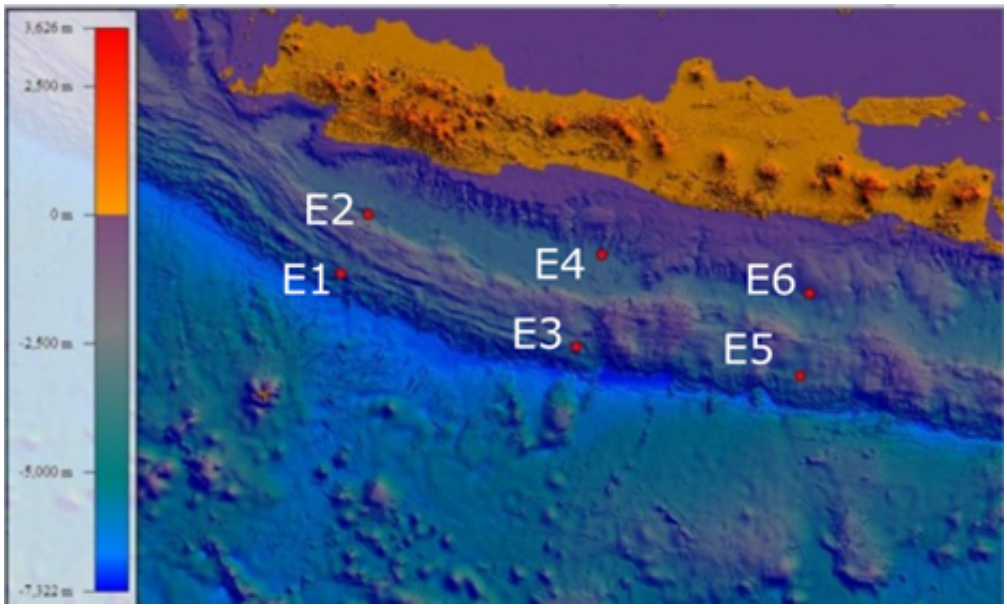

Figure 1: Modeling Area Boundaries and Earthquake Epicenters

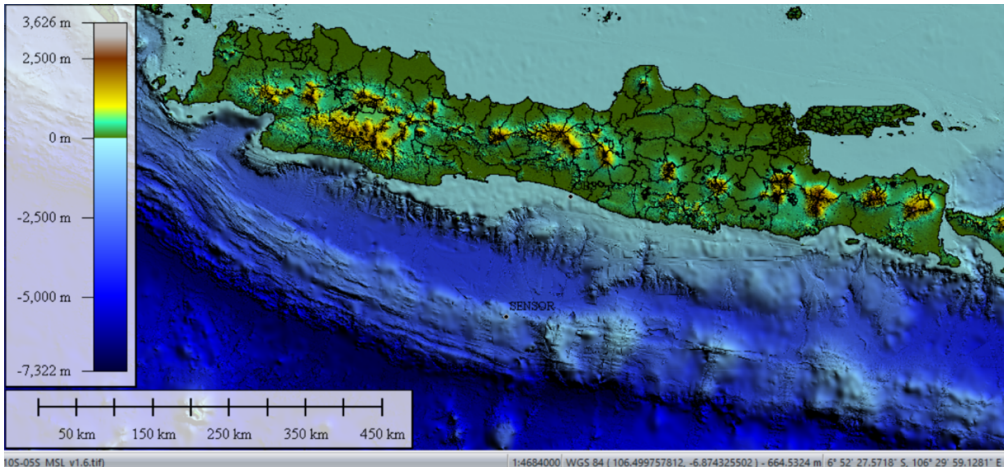

Figure 2: Observation and Sensor Points Near Yogyakarta International Airport (YIA)

Initial Water Surface Deformation

Using the earthquake parameters from each scenario, the initial seafloor deformation was computed through the multi-deformation method. This deformation forms the initial condition for the tsunami simulation in TUNAMI F1. Figure 3 provides examples of initial water surface conditions for the six epicenter groups.

2.2 TUNAMI F1 Modeling

Numerical modeling using TUNAMI F1 is a linear model simulated for 2 hours or 7200 seconds with a 30-second interval. The tsunami sea surface height modeling using TUNAMI F1 generates the maximum water surface height and the wave arrival time at the observation points.

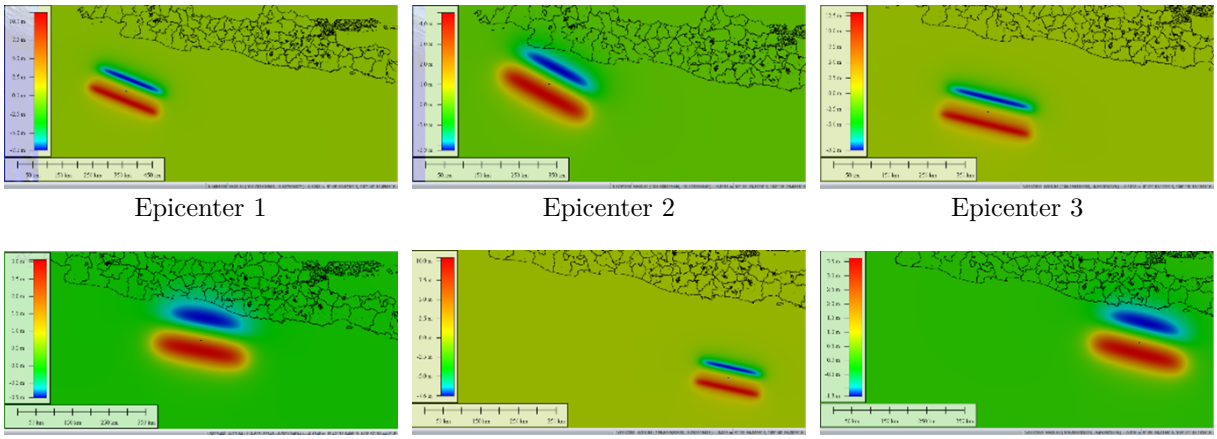

Epicenter 1 | Epicenter 2 | Epicenter 3

Epicenter 4 | Epicenter 5 | Epicenter 6

Figure 3: Initial Water Surface Conditions for the Six Epicenter Groups

The simulation of tsunami wave propagation characteristics with TUNAMI F1 uses several input data, including bathymetric data, which are converted into a spacing grid of 185 meters (0.0016667 arc degrees), source data (initial tsunami height values), observation points, and sensor points with a Geographic coordinate system (Longitude/Latitude). Table 3 shows the settings for the TUNAMI F1 model simulation.

The mass conservation and momentum equations describe three-dimensional shallow-water wave propagation. Following [8], the governing equations are given in Equations 1–4.

$$\frac{\partial \eta}{\partial t} + \frac{\partial u}{\partial x} + \frac{\partial v}{\partial y} + \frac{\partial w}{\partial z} = 0 \tag{1}$$

$$\frac{\partial u}{\partial t} + u\frac{\partial u}{\partial x} + v\frac{\partial u}{\partial y} + w\frac{\partial u}{\partial z} + \frac{1}{\rho}\frac{\partial p}{\partial x} + \frac{1}{\rho}\left(\frac{\partial \tau_{xx}}{\partial x} + \frac{\partial \tau_{xy}}{\partial y} + \frac{\partial \tau_{xz}}{\partial z}\right) = 0 \tag{2}$$

$$\frac{\partial v}{\partial t} + u\frac{\partial v}{\partial x} + v\frac{\partial v}{\partial y} + w\frac{\partial v}{\partial z} + \frac{1}{\rho}\frac{\partial p}{\partial y} + \frac{1}{\rho}\left(\frac{\partial \tau_{xy}}{\partial x} + \frac{\partial \tau_{yy}}{\partial y} + \frac{\partial \tau_{yz}}{\partial z}\right) = 0 \tag{3}$$

$$g + \frac{1}{\rho}\frac{\partial p}{\partial z} = 0 \tag{4}$$

The variables used in the governing equations are defined as follows. The symbol t denotes time, while η represents the change in water surface elevation and h denotes the water depth. The quantities u, v, and w correspond to particle velocities in the x, y, and z directions, respectively. The parameter g is the gravitational acceleration, and τ_{ij} indicates the normal or tangential stress acting in the i-direction on the plane with orientation j.

The vertical momentum equation, combined with the surface boundary condition where the pressure is zero ($p = 0$), leads to the hydrostatic pressure relation $p = \rho g(\eta - z)$. To solve the mass conservation equation, dynamic and kinematic boundary conditions are imposed at both the free surface and the seabed. At the free surface, the pressure must vanish, as expressed in Equation 5. The kinematic conditions relate the vertical velocity w to the time rate of change and horizontal gradients of the free-surface elevation, as shown in Equations 6 and 7.

$$p = 0 \qquad \text{at } z = \eta \tag{5}$$

$$w = \frac{\partial \eta}{\partial t} + u\frac{\partial \eta}{\partial x} + v\frac{\partial \eta}{\partial y} \qquad \text{at } z = \eta \tag{6}$$

$$w = -u\frac{\partial \eta}{\partial x} + v\frac{\partial \eta}{\partial y} \qquad \text{at } z = \eta \tag{7}$$

The symbols used in these boundary conditions are defined as follows: η denotes the water surface elevation, ρ is the fluid density, and p represents the hydrostatic pressure.

By integrating the vertical momentum equation from the free surface to the seabed using Leibniz's rule, the governing equations reduce to the depth-integrated shallow-water system expressed in terms of flux (or volume flow). This formulation yields the two-dimensional continuity and momentum equations shown in Equations 8–10. These equations describe the evolution of the free-surface elevation and the corresponding mass fluxes M and N in the horizontal directions.

$$\frac{\partial \eta}{\partial t} + u\frac{\partial M}{\partial x} + v\frac{\partial N}{\partial y} = 0 \tag{8}$$

$$\frac{\partial M}{\partial t} + \frac{\partial}{\partial x}\left(\frac{M^2}{D}\right) + \frac{\partial}{\partial y}\left(\frac{MN}{D}\right) + gD\frac{\partial \eta}{\partial x} + \frac{\tau_x}{\rho} = A\left(\frac{\partial^2 M}{\partial x^2} + \frac{\partial^2 M}{\partial y^2}\right) \tag{9}$$

$$\frac{\partial N}{\partial t} + \frac{\partial}{\partial x}\left(\frac{MN}{D}\right) + \frac{\partial}{\partial y}\left(\frac{N^2}{D}\right) + gD\frac{\partial \eta}{\partial y} + \frac{\tau_y}{\rho} = A\left(\frac{\partial^2 N}{\partial x^2} + \frac{\partial^2 N}{\partial y^2}\right) \tag{10}$$

In these equations, $D = h + \eta$ denotes the total water depth, while τ_x and τ_y represent the bottom friction in the x- and y-directions. The parameter A is the eddy viscosity coefficient, assumed constant, and wind-induced surface stress is neglected. The flux terms M and N correspond to depth-integrated discharges in the horizontal directions and are defined as:

$$M = \int_{-h}^{\eta} u\, dz = u(h + \eta) = uD \tag{11}$$

$$N = \int_{-h}^{\eta} v\, dz = v(h + \eta) = vD \tag{12}$$

Based on the earthquake scenarios defined earlier, the TUNAMI F1 model was executed 36 times to generate the corresponding tsunami simulations. Each simulation produced a pair of output files containing the maximum Sea Surface Height (SSH) and the Estimated Tsunami Arrival Time (ETATSU), which were compiled as the primary dataset for developing and validating the fuzzy logic early warning model. The overall simulation workflow is illustrated in Figure 4, while the numerical configuration of the TUNAMI F1 model—including grid resolution, spatial spacing, and time-stepping parameters—is summarized in Table 3.

Table 3: TUNAMI F1 Model Simulation Settings

Grid Size		Spacing Grid	Time Step	Total Time Simulation	Interval
X	Y				
655	324	1.0	2.0	7200	60

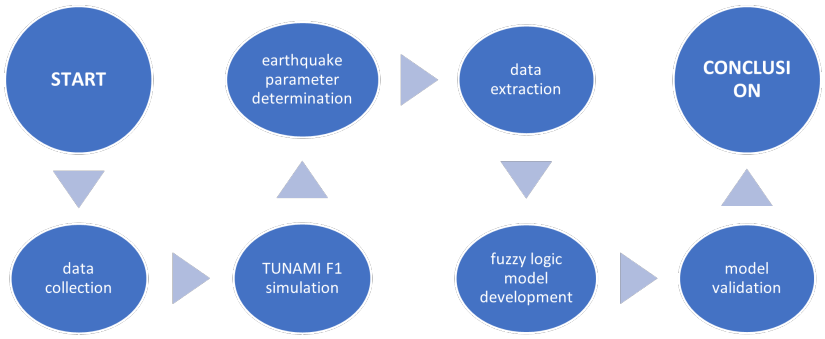

Figure 4: Research Method Flowchart

3 Results and Discussion

The results of running the TUNAMI F1 model 36 times are presented below. This simulation was designed to test the effectiveness of an early warning system by establishing two different types of data collection locations:

1. **Observation Points:** These points represent critical locations on the coast (beach) where the actual impact or `ground truth` of the tsunami is measured. The Sea Surface Height (SSH) and Estimated Time of Arrival (ETA) data at these points are considered the real impact that will occur on land.
2. **Sensor Points:** These points are positioned offshore, simulating the location of tsunami detection buoys (such as the DART system). These points are designed to capture tsunami wave data *before* it reaches the coast, thus serving as the data source for the early warning system.

The purpose of this analysis is to determine whether the data collected at the *Sensor Points* can be used to accurately predict the tsunami characteristics (especially SSH) at the *Observation Points*.

The data above serves as the basis for determining the membership functions in the fuzzy logic model. This fuzzy logic model aims to compare whether the early warning system generated by the fuzzy logic simulation at the sensor point corresponds to the actual tsunami sea surface height at the observation point. Therefore, the analysis focuses on the data at the sensor points.

The input parameters used to model fuzzy logic in this study are ETATSU and SSH. Therefore, membership functions (MEFs) are needed to categorize the data into groups. For SSH or tsunami sea surface height, the membership function has been determined by BMKG [12], as shown in (Figure 5). However, for ETATSU, no official authority has established a membership function, so its determination is based on expert judgment. The ETATSU membership function is limited to a time range of 50 minutes and divided into three categories: fast, moderate, and slow (Figure 6). Subsequently, to implement the fuzzy logic model, a set of rules must be created, enabling the fuzzy logic model to run and complete the data processing phase.

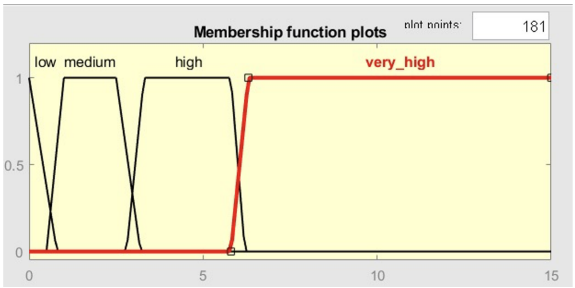

Figure 5: MEF sea surface height

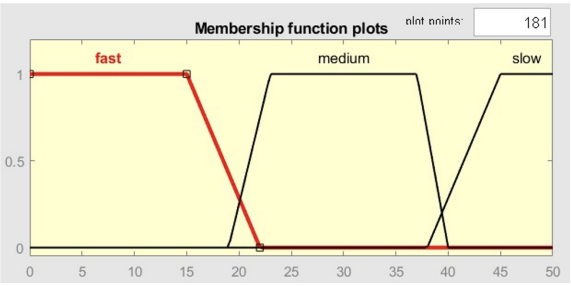

Figure 6: MEF ETATSU

The fuzzy logic model demonstrated a high overall accuracy of 83.3% across the 36 simulated scenarios, successfully classifying tsunami risk into 'WASPADA' (Advisory), 'SIAGA' (Warning), and 'AWAS' (Major Warning) categories. However, this overall figure masks a critical underlying pattern: the model's performance was not uniform across different source locations.

A deeper analysis reveals a stark performance divide. The model achieved a 100% success rate for all magnitudes originating from `Epicenter 1` and `Epicenter 6`. Conversely, all classification errors occurred in scenarios from `Epicenter 2, 3, 4,` and `5`, particularly at high magnitudes (Mw 8.2 and 8.5). This pattern strongly suggests that a `one-size-fits-all` fuzzy model is insufficient. The relationship between the tsunami parameters at the offshore *Sensor Point* and the coastal *Observation Point* is not a simple, universal constant; it is highly dependent on the local bathymetry and coastal geometry of each specific path.

Table 4: ETATSU and SSH Data for 36 Tsunami Scenarios

No.	Source	Mag.	Code	Observation Points		Sensor Points	
				ETA (min)	SSH (m)	ETA (min)	SSH (m)
1	1	7	E1M70	54	0,06	24	0,03
2	1	7,3	E1M73	53	0,13	24	0,06
3	1	7,6	E1M76	52	0,27	22	0,16
4	1	7,9	E1M79	51	0,56	21	0,32
5	1	8,2	E1M82	49	2,15	19	0,49
6	1	8,5	E1M85	47	4,03	17	0,96
7	2	7	E2M70	70	0,03	27	0,01
8	2	7,3	E2M73	49	0,09	24	0,03
9	2	7,6	E2M76	52	0,27	22	0,16
10	2	7,9	E2M79	46	0,44	21	0,18
11	2	8,2	E2M82	44	0,85	19	0,21
12	2	8,5	E2M85	42	1,27	16	0,68
13	3	7	E3M70	42	0,15	13	0,04
14	3	7,3	E3M73	42	0,39	12	0,09
15	3	7,6	E3M76	41	0,86	11	0,19
16	3	7,9	E3M79	41	1,69	10	0,51
17	3	8,2	E3M82	40	3,28	8	1,28
18	3	8,5	E3M85	38	9,65	5	3,17
19	4	7	E4M70	21	0,10	3	0,02
20	4	7,3	E4M73	21	0,29	1	0,06
21	4	7,6	E4M76	21	0,69	0	0,13
22	4	7,9	E4M79	21	1,66	0	0,35
23	4	8,2	E4M82	21	3,38	0	0,82
24	4	8,5	E4M85	21	5,62	0	1,70
25	5	7	E5M70	51	0,12	26	0,07
26	5	7,3	E5M73	51	0,28	25	0,12
27	5	7,6	E5M76	49	0,58	24	0,29
28	5	7,9	E5M79	48	1,02	22	0,51
29	5	8,2	E5M82	45	1,78	20	0,76
30	5	8,5	E5M85				
31	6	7	E6M70	79	0,04	Not reached	0,01
32	6	7,3	E6M73	42	0,04	30	0,02
33	6	7,6	E6M76	40	0,09	26	0,05
34	6	7,9	E6M79	37	0,19	23	0,10
35	6	8,2	E6M82	30	0,55	20	0,20
36	6	8,5	E6M85	29	0,79	16	0,46

For Epicenters 1 and 6, the local geography may result in a simple, linear relationship (e.g., a 1m wave at the sensor consistently becomes a 1.5m wave at the coast). The fuzzy model was able to successfully learn this simple rule. However, for Epicenters 2–5, the undersea topography (such as submarine canyons or shallow reefs) likely causes complex, *non-linear amplification effects*. This is the critical insight:

- Scenario E3M85 (Mw 8.5): A 3.17m wave at the sensor (already 'AWAS') is amplified nearly 300% to 9.65m at the coast.
- Scenario E4M85 (Mw 8.5): A 1.70m wave at the sensor ('SIAGA') is amplified 330% to 5.62m at the coast ('AWAS').

The model's errors are directly traceable to this non-linear amplification. The model's most significant failures occurred when it saw a sensor reading that, for most epicenters, would be correct, but for that specific location, was a severe underestimation.

For example, the error in Scenario E2M85 (Mw 8.5)—which the analysis noted as 'invalid'—is particularly illuminating. The sensor recorded only 0.68m (a 'SIAGA' level event), while the

coast experienced 1.27m (also 'SIAGA'). The model likely classified the 0.68m sensor reading as 'WASPADA' based on its rules, failing to account for the 187% amplification specific to that path. This is a classic *classification failure*, where the model's generalized rules were incorrect for a specific, complex case.

This is distinct from the issue in Scenario E5M85, where the simulation data itself was missing (see Table 4). *This is a simulation or input data failure*, not a failure of the fuzzy logic model itself, and must be treated as a null point in the accuracy calculation.

The analysis demonstrates that the primary limitation of the current model is its lack of spatial awareness. It only considers what the wave height is, not where it is coming from and how the local geography will transform it. This finding aligns with previous studies [1] but adds a crucial, specific recommendation. Future work should move beyond simply refining membership functions. To be effective, the model must:

- `Develop Location-Specific Models:` Instead of one generic model, location-specific fuzzy models (or 'fuzzy rule-sets') should be developed for different coastal segments, each tuned to its unique bathymetric profile.
- `Incorporate a New Input Variable:` A more robust model would integrate a new input variable, such as a 'Local Amplification Factor' (LAF). This (pre-calculated) factor would represent the specific amplification properties of the bathymetry between a given sensor and a given observation point, allowing the model to dynamically adjust its warning level.

4 Conclusion

This study developed a fuzzy logic model for a tsunami early warning system by incorporating maximum sea surface height and estimated arrival time. The model is integrated with TUNAMI F1 simulations, which account for fluid dynamics and seabed topography.

The simulation results indicate that the model achieved an overall accuracy of 83.3%, with the highest success rates observed in the first and sixth epicenters. However, the model exhibited errors in several high-magnitude scenarios (Mw $\geq$ 8.5), highlighting the need for further improvements in defining membership functions and input parameters.

This study enhances the effectiveness of tsunami early warning systems through a fuzzy logic–based approach. For future development, it is recommended to integrate additional parameters such as local bathymetric effects and coastline variability and perform validation using historical tsunami data to improve the model's accuracy and reliability.

In conclusion, while this study confirms the potential of fuzzy logic, it critically highlights that tsunami early warning is not just a magnitude problem; it is a location problem. A reliable system must account for this complex, location-dependent amplification.

CRediT Authorship Contribution Statement

Sadiyana Yaqutna Naqiya: Conceptualization; methodology; numerical simulation; data curation; formal analysis; writing–original draft preparation. **Hanah Khoirunnisa**: Validation; investigation; hydrodynamic modeling supervision; resources; writing–review and editing. **Galih Pradananta**: Supervision; methodology refinement; project administration; visualization; writing–review and editing; corresponding author.

Declaration of Generative AI and AI-assisted Technologies

The authors declare that no generative AI or AI-assisted technologies were used in the writing, analysis, or preparation of this manuscript. All text, data analyses, simulations, figures, and interpretations were produced manually by the authors. Any software used (e.g., TUNAMI

F1, GIS tools, numerical solvers) served only for standard scientific computation and not for generative content creation.

Declaration of Competing Interest

The authors declare that they have no known competing financial interests or personal relationships that could have appeared to influence the work reported in this paper.

Funding and Acknowledgments

This research received no specific grant from any funding agency in the public, commercial, or not-for-profit sectors. The authors gratefully acknowledge the support of the Research Center for Hydrodynamics (BRIN), BMKG for tsunami early-warning parameter references, and access to bathymetry data from Batimetri Nasional (BatNas). The authors also thank all institutions and colleagues who provided scientific input during the simulation and analysis stages.

Data and Code Availability

The datasets generated and analyzed during this study, including the 36 TUNAMI F1 simulation outputs (SSH and ETATSU), are available from the corresponding author upon reasonable request. The numerical modeling scripts used to process the simulation results are also available upon request, subject to institutional data-sharing policies.

References

[1] B. Qayyum, A. Ahmed, I. Ullah, and S. A. Shah, "A fuzzy-logic approach for optimized and cost-effective early warning system for tsunami detection," *Sustainability*, vol. 14, no. 21, p. 14 516, 2022. DOI: 10.3390/su142114516.

[2] D. P. Setyaningsih et al., "Tsunami hazard modeling in the coastal area of kulon progo regency," *International Journal of Remote Sensing and Earth Sciences (IJReSES)*, vol. 19, no. 2, p. 184, 2023. DOI: 10.30536/j.ijreses.2022.v19.a3822.

[3] S. G. Dheeban, A. Gangadharan, and S. G. Vaidyanathan, "Fuzzy alert: An intelligent alert mechanism for tsunami," in *Proceedings of the 5th International Conference on Information Technology and Applications (ICITA)*, 2008. Available online.

[4] A. Ghosh and P. Dey, "Flood severity assessment of the coastal tract situated between muriganga and saptamukhi estuaries of sundarban delta of india using fr, fl, lr and rf models," *Regional Studies in Marine Science*, vol. 42, p. 101 624, 2021. DOI: 10.1016/j.rsma.2021.101624.

[5] S. M. Agayan, S. R. Bogoutdinov, R. I. Krasnoperov, O. V. Efremova, and D. A. Kamaev, "Fuzzy logic methods in the analysis of tsunami wave dynamics based on sea level data," *Pure and Applied Geophysics*, vol. 179, no. 11, pp. 4053–4062, 2022. DOI: 10.1007/s00024-022-03104-x.

[6] B. Aydın, S. Yağuzluk, and M. Açıkkar, "Prediction of landslide tsunami run-up on a plane beach through feature selected mlp-based model," *Journal of Ocean Engineering and Science*, vol. 9, no. 3, pp. 222–231, 2024. DOI: 10.1016/j.joes.2022.05.007.

[7] Y. Oishi, F. Imamura, and D. Sugawara, "Near-field tsunami inundation forecast using the parallel tunami-n2 model: Application to the 2011 tohoku-oki earthquake combined with source inversions," *Geophysical Research Letters*, 2015. DOI: 10.1002/2014GL062577.

[8] F. Imamura, A. C. Yalçiner, and G. Ozyurt, *Tsunami Modelling Manual*. 2006. Available online.

[9] A. Rashidi, Z. H. Shomali, D. Dutykh, and N. Keshavarz Faraj Khah, "Evaluation of tsunami wave energy generated by earthquakes in the makran subduction zone," *Ocean Engineering*, vol. 165, pp. 131–139, 2018. DOI: 10.1016/j.oceaneng.2018.07.027.

[10] E. Zhao, Y. Wu, F. Jiang, Y. Wang, Z. Zhang, and C. Nie, "Numerical investigation on the influence of the complete tsunami-like wave on the tandem pipeline," *Ocean Engineering*, vol. 294, p. 116 697, 2024. DOI: 10.1016/j.oceaneng.2024.116697.

[11] D. L. Wells and K. J. Coppersmith, "New empirical relationships between magnitude, rupture length, rupture width, rupture area, and surface displacement," *Bulletin of the Seismological Society of America*, vol. 84, no. 4, pp. 974–1002, 1994. Available online.

[12] Badan Meteorologi Klimatologi dan Geofisika, *Peraturan Kepala BMKG Nomor 07 Tahun 2019 tentang Pedoman Implementasi Sistem Peringatan Dini Tsunami*. Jakarta: BMKG, 2019. Available online.